# Interchannel-coupling effects in the spin polarization of energetic photoelectrons

Himadri S. Chakraborty,[1,2] Pranawa C. Deshmukh,[3] and Steven T. Manson[4]
[1]*Max-Planck-Institut für Physik Komplexer Systeme, Nöthnitzer Strasse 38, D-01187 Dresden, Germany*
[2]*James R. Macdonald Laboratory, Department of Physics, Kansas State University, Manhattan, Kansas 66506-2604*
[3]*Department of Physics, Indian Institute of Technology-Madras, Chennai 600036, India*
[4]*Department of Physics and Astronomy, Georgia State University, Atlanta, Georgia 30303-3083*
(Received 24 January 2003; published 6 May 2003)

Effects of the interchannel coupling on the spin polarization of energetic photoelectrons emitted from atomic Ne valence subshells are examined. Like previously obtained results for cross sections and angular distributions, the photoelectron spin polarization parameters too are found considerably influenced by the coupling. The result completes a series of studies to finally conclude that the independent particle description is inadequate for the *entire* range of photoionization dynamics over the *full* spectral energy domain.

DOI: 10.1103/PhysRevA.67.052701 PACS number(s): 32.80.Fb, 32.80.Hd

## I. INTRODUCTION

The study of the spin polarization of photoelectrons is important primarily on two counts. First, since this effect originates from purely relativistic interactions, its behavior provides insights into relativistic aspects of the dynamical correlation, which are inaccessible by conventional studies of cross section and angular distribution; in the photoionization of lighter atoms, which may normally seem tractable by a nonrelativistic approach, sizable resonance features in spin-polarization spectra of emerging electrons can be found when relativistic forces are included [1,2]. Second, spin resolved spectroscopic measurements in conjunction with cross section and angular distribution data provide a comprehensive methodology to *completely* characterize the photoionization process [3,4]. As a virtual beginning of the interest in the field, the emission of highly spin-polarized electrons over a limited range of the ejection angle near the Cooper minimum of the photoionization cross section was predicted by Fano many years ago [5]. Since then, the spin polarization of photoelectrons emanating from unpolarized atoms has been the subject of several theoretical and experimental investigations (for reviews see Refs. [6,7]). However, the focus of all these studies has been the low photon energy range (vuv and soft x-ray), over which it is a common knowledge that the electron correlation, in its complete form including interchannel coupling, is significant and often dominating.

On the other hand, at photon energies far away from the ionization threshold, it was believed until recently that the independent particle (IP) framework, which completely disregards electron correlation, can adequately describe the photoionization process [8–13]. However, over a series of combined experimental and theoretical studies this notion has recently been corrected for the cross section and the angular distribution asymmetry parameter [14–16]. Interchannel coupling has been shown to be a crucial determinant of the quantitative accuracy of these parameters in the intermediate and the high-energy regime for photoelectrons emitted from both inner and outer atomic subshells. From a perturbative perspective, the effect originates from the correction to the single channel matrix element from a continuum configuration interaction among all neighboring channels [14]. Since the dynamical difference among relativistic (spin-orbit) channels arising from a given subshell determines the spin-polarization character of electrons photoejected from that subshell, it is of particular interest to examine how the spin-polarization parameters are affected by correlation in the form of interchannel coupling mechanism. In this paper, we focus on this aspect by investigating the spin-polarization parameters of the valence $2p$ photoelectrons from atomic Ne.

## II. ESSENTIAL THEORETICAL DETAILS

The relativistic-random phase approximation (RRPA) [17,18] has been employed to perform the calculation. The RRPA calculation starts from an explicitly relativistic basis so that relativistic interactions are included *ab initio*. In addition to the ground-state correlation, as well as two-electron promotion in the residual Ne-ion core, RRPA incorporates interchannel coupling among *all* of the single excitation/ionization final state channels. We use a framework in which the coupling among selective members of the relativistic dipole-allowed $jj$-coupled channels:

$$1s_{1/2}\rightarrow kp_{3/2},kp_{1/2}, \quad 2s_{1/2}\rightarrow kp_{3/2},kp_{1/2}, \tag{1}$$

$$2p_{1/2}\rightarrow kd_{3/2},ks_{1/2}, \quad \text{and} \quad 2p_{3/2}\rightarrow kd_{5/2},kd_{3/2},ks_{1/2}$$

can be chosen. The calculation has been carried out in both the length and the velocity gauge formalism; the good agreement between length and velocity results, even at highest photon energy considered, indicates the numerical accuracy of our calculation. It may be mentioned here that RRPA has been used previously with reasonable success to study the spin polarization of photoelectrons from noble gases, but only in the low photon energy range [19].

In this calculation, we have considered the case where the target atom is unpolarized and the polarization of the residual ion is not observed. Equivalently, the polarization of the target atom is averaged out and that of the residual ion is summed over. The dipole photoionization can then be *completely* described, in general, by a set of five dynamical pa-

 

rameters $\sigma$, $\beta$, $\xi$, $\eta$, and $\zeta$, wherein $\sigma$ is the partial cross section, $\beta$ is the angular distribution asymmetry parameter and the others are the photoelectron spin-polarization parameters. These dynamical parameters can be expressed in terms of the reduced dipole matrix elements [17] of the process. The explicit expressions for the spin-polarization parameters corresponding to both $2p_{1/2}$ and $2p_{3/2}$ photoelectrons of Ne are given as [20]

$$\xi_{2p_{3/2}}=\left[\frac{1}{2}|D_{s_{1/2}}|^2+\frac{2}{5}|D_{d_{3/2}}|^2-\frac{9}{10}|D_{d_{5/2}}|^2 - \frac{\sqrt{5}}{2}|D_{s_{1/2}}||D_{d_{3/2}}|\cos(\theta_{s_{1/2}}-\theta_{d_{3/2}}) + \frac{9}{10}|D_{d_{3/2}}||D_{d_{5/2}}|\cos(\theta_{d_{3/2}}-\theta_{d_{5/2}})\right]\bar{\sigma}^{-1}_{2p_{3/2}}, \quad (2a)$$

$$\xi_{2p_{1/2}}=\left[-|D_{s_{1/2}}|^2+|D_{d_{3/2}}|^2-\frac{1}{\sqrt{2}}|D_{s_{1/2}}||D_{d_{3/2}}| \times\cos(\theta_{s_{1/2}}-\theta_{d_{3/2}})\right]\bar{\sigma}^{-1}_{2p_{1/2}}, \quad (2b)$$

$$\eta_{2p_{3/2}}=\left[-\frac{3}{2}\sqrt{\frac{1}{5}}|D_{s_{1/2}}||D_{d_{3/2}}|\sin(\theta_{s_{1/2}}-\theta_{d_{3/2}}) +3\sqrt{\frac{1}{5}}|D_{s_{1/2}}||D_{d_{5/2}}|\sin(\theta_{s_{1/2}}-\theta_{d_{5/2}}) -\frac{3}{2}|D_{d_{3/2}}||D_{d_{5/2}}|\sin(\theta_{d_{3/2}}-\theta_{d_{5/2}})\right]\bar{\sigma}^{-1}_{2p_{3/2}}, \quad (3a)$$

$$\eta_{2p_{1/2}}=\left[\frac{3}{\sqrt{2}}|D_{s_{1/2}}||D_{d_{3/2}}|\sin(\theta_{s_{1/2}}-\theta_{d_{3/2}})\right]\bar{\sigma}^{-1}_{2p_{1/2}}, \quad (3b)$$

$$\zeta_{2p_{3/2}}=\left[-\frac{1}{2}|D_{s_{1/2}}|^2+\frac{1}{5}|D_{d_{3/2}}|^2+\frac{3}{10}|D_{d_{5/2}}|^2 -\sqrt{5}|D_{s_{1/2}}||D_{d_{3/2}}|\cos(\theta_{s_{1/2}}-\theta_{d_{3/2}}) -\frac{9}{5}|D_{d_{3/2}}||D_{d_{5/2}}|\cos(\theta_{d_{3/2}}-\theta_{d_{5/2}})\right]\bar{\sigma}^{-1}_{2p_{3/2}}, \quad (4a)$$

$$\zeta_{2p_{1/2}}=\left[|D_{s_{1/2}}|^2+\frac{1}{2}|D_{d_{3/2}}|^2-\sqrt{2}|D_{s_{1/2}}||D_{d_{3/2}}| \times\cos(\theta_{s_{1/2}}-\theta_{d_{3/2}})\right]\bar{\sigma}^{-1}_{2p_{1/2}}, \quad (4b)$$

where, with the photon energy $\omega$, the subshell cross sections are

$$\sigma_{2p_{3/2}}=\frac{8\pi^4}{\omega c}\bar{\sigma}_{2p_{3/2}}=\frac{8\pi^4}{\omega c}[|D_{s_{1/2}}|^2+|D_{d_{3/2}}|^2+|D_{d_{5/2}}|^2], \quad (5a)$$

$$\sigma_{2p_{1/2}}=\frac{8\pi^4}{\omega c}\bar{\sigma}_{2p_{1/2}}=\frac{8\pi^4}{\omega c}[|D_{s_{1/2}}|^2+|D_{d_{3/2}}|^2]. \quad (5b)$$

In the above equations we use the shorthand notations $D_{l'_{j'}}$ and $\theta_{l'_{j'}}$ for the reduced matrix element $D_{nl_j\to kl'_{j'}}$ and the phase shift $\theta_{nl_j\to kl'_{j'}}$, respectively, corresponding to the $nl_j \to kl'_{j'}$ dissociation channel. Conventionally, additional parameters $\delta_{nl_j}=(\zeta_{nl_j}-2\xi_{nl_j})/3$ are also used, which connect to the spin polarization of the total photoelectron flux [20].

## III. RESULTS AND DISCUSSION

In order to uncover the details of how the interchannel coupling influences the photoelectron spin-polarization dynamics we have performed five separate calculations for the $2p_{3/2}$ and $2p_{1/2}$ photoionization of Ne with varying degrees of interchannel coupling. These are (1) no interchannel coupling among channels arising from different relativistic subshells, (2) coupling of all channels from $2p_{3/2}$ and $2p_{1/2}$ subshells, (3) from $2p$ and $2s$ subshells, (4) from $2p$ and $1s$ subshells, and (5) from all four subshells together (full calculation). Since, in calculation (1), we ignore all effects of interchannel coupling between channels arising from differing relativistic subshells, this is similar to the relativistic IP description, except that ground-state correlations are included along with coupling among channels arising from the same subshell.

An elegant approach to understand the relative importance of the coupling with different neighboring channels has been described in Ref. [14] in the spirit of a first-order perturbation theory. Under the influence of a perturbing degenerate channel $J$ the corrected wave functions $\Psi_{2p_j}$ for any dipole channel $2p_j\to ks_{1/2}(kd_{j'})$ [see Eq. (1)] from either of $2p_j(j=1/2,3/2)$ subshells are given, at the photoelectron kinetic energy $E$, by

$$\Psi_{2p_j}(E)=\psi_{2p_j}(E) + \int \frac{\langle\psi_J(E')|H-H_0|\psi_{2p_j}(E)\rangle}{E-E'}\psi_J(E')dE', \quad (6)$$

where $\psi$'s denote unperturbed wave functions, which are eigenfunctions of the unperturbed Hamiltonian $H_0$, and the final state total angular momentum $j'$ has two dipole-allowed values 5/2 and 3/2. In Eq. (6), the matrix element under the energy integration is the interchannel coupling matrix element with $H$ being the *full* Hamiltonian of the system. Now, defining the dipole photoionization matrix element for $2p_j\to ks_{1/2}(kd_{j'})$ transitions with no interchannel coupling

among channels arising from different relativistic subshells, corresponding to calculation (1), as

$$D_{2p_j}(E)=\langle\psi_i|T|\psi_{2p_j}(E)\rangle, \tag{7}$$

with $\psi_i$ being the ground-state wave function and $T$ the transition operator, the corresponding perturbed matrix elements can be expressed as

$$M_{2p_j}(E)=D_{2p_j}(E)+\int \frac{\langle\psi_J(E')|H-H_0|\psi_{2p_j}(E)\rangle}{E-E'}D_J(E')dE'. \tag{8}$$

The correction term on the right side of Eq. (8) can be significant if two conditions are simultaneously satisfied. First, the spatial overlap between the perturbed and perturbing channel wave functions must be considerable to result in a significant interchannel coupling matrix element; this is expected when the discrete wave functions have the same principal quantum numbers so that they occupy the same region of space and have significant overlap, and the respective ionization thresholds are close so that at high enough energies the electrons from both subshells have similar momenta, which enable the continuum wave functions to oscillate roughly ''in phase.'' Second, the magnitude of the unperturbed matrix element of the perturbing channel is considerably larger than that of the perturbed channel. Now the form of the energy integral suggests that the primary contribution of interchannel interaction will come from the values of the integrand at $E'\simeq E$. Importantly further, the electron continuum wave functions, participating in the energy integral, must be normalized per unit energy through a multiplication by a factor $m\hbar^{-2}E^{-1/4}$ [21]. Therefore, the leading energy behavior of the interchannel coupling matrix element in Eq. (6) turns out to be $E^{-1/2}$ when the energy is high enough. Evidently, considering Eq. (8), if the uncoupled matrix element $D_J$ of channel $J$ decreases with energy slower by a factor $E^{1/2}$ or more than the corresponding decay of $D_{2p_j\rightarrow ks_{1/2}(kd_{j'})}$, the resulting effect of the coupling will be considerable, provided the interchannel coupling matrix element is significant. Indeed, this leads us to expect a strong effect of the $2s$ channels (with Dirac-Fock threshold 52.68 eV) on $2p_j$ photoionization (with thresholds 23.08 eV for $j=3/2$ and 23.21 eV for $j=1/2$). This is clearly seen in Fig. 1, which gives our calculated results for the $2p_{1/2}$ and the $2p_{3/2}$ subshell cross sections in each of the five calculations described above; at the highest energies, the cross section results are seen to essentially coalesce into just two curves—those including coupling between and those omitting that coupling from the other. This was noted previously in Ref. [14] where similar calculations were performed. Because the high energy uncoupled photoionization cross section for an *nl* subshell falls off with energy as $E^{-(7/2+l)}$, the correction term in Eq. (8) falls off in the limit of $\omega\rightarrow E$, as $E^{-(5/4+l/2)}$) [22]. As applied to the present case, the perturbation of $D_{2p_j}$ by $D_{2s}$ falls off as $E^{-(5/4+l/2)}$, the same as the falloff of the $D_{2p_j}$ themselves, so that the perturbation is of the same order of size as the uncoupled matrix elements. The weak effect of $1s$ channels on either of $2p_j$ cross sections, as also seen in Fig. 1, is owing to the much higher $1s$ ionization threshold (893.02 eV) that results in poor overlap of the continuum wave functions in ensuing interchannel coupling matrix element, along with the fact that the discrete $1s$ and $2p_j$ wave functions occupy very different regions of space and, therefore, overlap poorly.

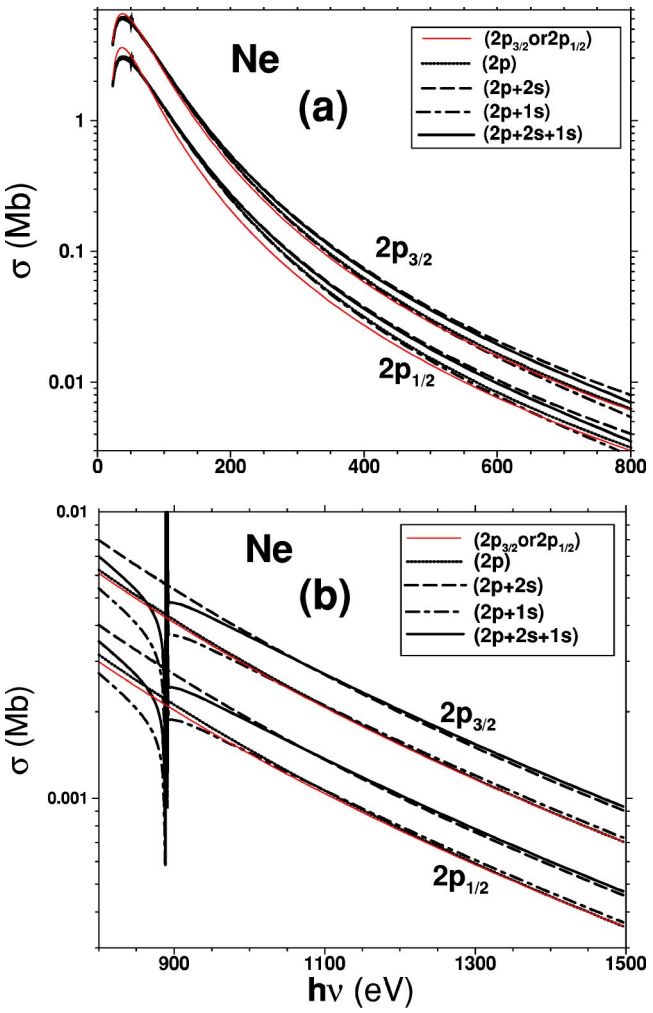


FIG. 1. Ne $2p_{3/2}$ and $2p_{1/2}$ spin-orbit subshell cross sections in several selections of channels calculated by the relativistic-random phase approximation: (a) for photon energy up to 800 eV and (b) from 800 eV to 1.5 KeV. The structure around 900 eV is due to $1s$ Rydberg resonances.

In addition, what is rather interesting to note in Fig. 1 is the tiny effect from the coupling between the channels from the spin-orbit split $2p_j$ subshells. The curve (thin solid) corresponding to only-$2p_{3/2}$ or only-$2p_{1/2}$ channels [calculation (1), similar to the IP result] differs very little in the lower part of the energy range [Fig. 1(a)] when compared to the curve (dotted) from all $2p$ channels combined; however, both the curves practically merge together at higher energies [Fig. 1(b)] indicating virtually no effect from the coupling.

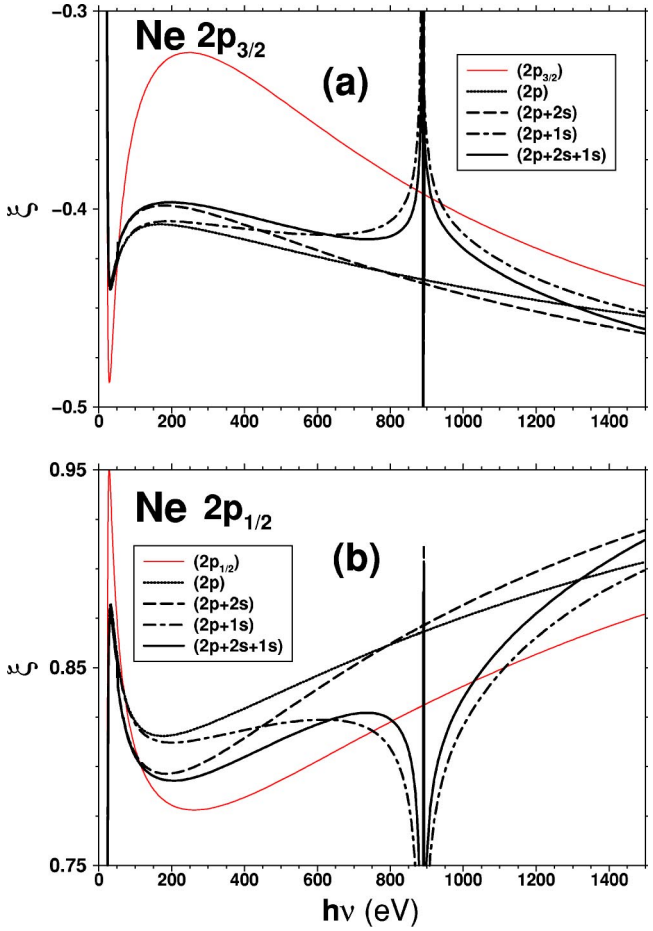


FIG. 2. Spin-polarization parameter $\xi$ for (a) $2p_{3/2}$ and (b) $2p_{1/2}$ photoelectrons calculated in the same selections of channels as in Fig. 1.

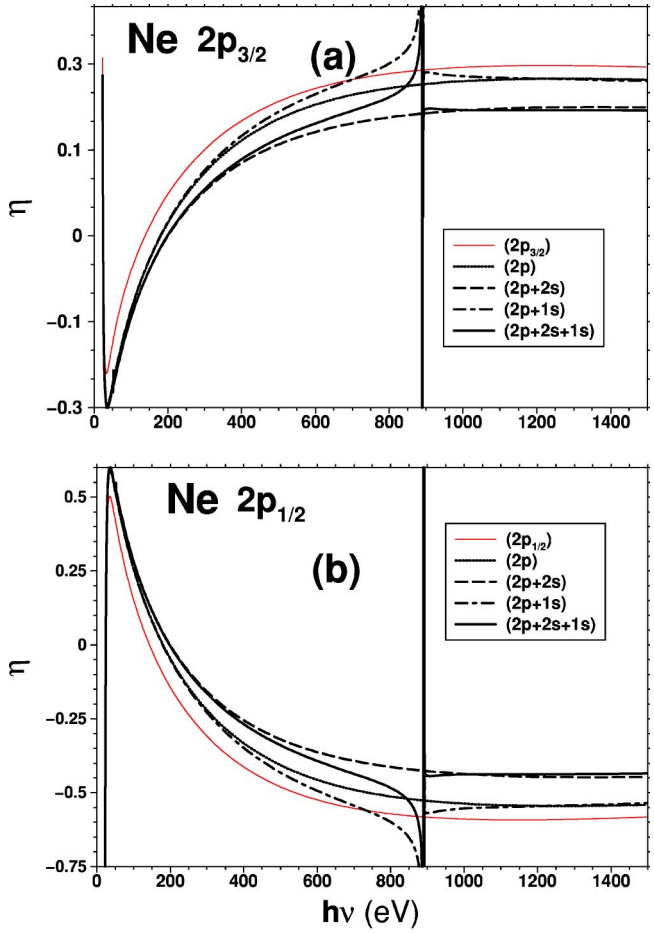


FIG. 3. Spin-polarization parameter $\eta$ for (a) $2p_{3/2}$ and (b) $2p_{1/2}$ photoelectrons.

This phenomenon can be understood as follows. It is true that the interchannel coupling matrix element between the $2p_{3/2}$ and $2p_{1/2}$ channels is strong due to the close proximity of their respective ionization thresholds. But since the high energy falloff of $D_{2p_{3/2}}$ and $D_{2p_{1/2}}$ are the same, the ensuing coupling corrections [Eq. (8)] fall off effectively as $E^{-1/2}$ at higher energy, explaining how the small coupling effect at lower energies becomes practically zero at higher energies.

Looking at our results for the spin-polarization parameters, Figs. 2–5, rather different phenomenology is evident; significant effects resulting from the coupling between the channels arising from the $2p_{3/2}$ and $2p_{1/2}$ spin-orbit subshells are noted. Understanding the underlying reason(s) for this phenomenology is somewhat more complex than for the cross sections owing to the fact that the spin-polarization parameters depend upon both the magnitudes *and* the phases of the dipole matrix elements, as seen from Eqs. (2)–(4). Thus, an understanding of the modification of the phase shifts engendered by interchannel coupling is also of importance.

Starting from Eq. (8) and explicitly introducing the unperturbed ($\theta$) and the perturbed ($\Theta$) phase shifts through the notations $D=|D|\exp(i\theta)$ and $M=|M|\exp(i\Theta)$ we obtain

$$\Theta_{2p_j}=\theta_{2p_j}-i\log\Bigg[\Bigg(|D_{2p_j}|(E)+\int\frac{\langle\psi_J(E')|H-H_0|\psi_{2p_j}(E)\rangle}{E-E'}|D_J|\times\exp[i(\theta_J-\theta_{2p_j})](E')dE'\Bigg)|M_{2p_j}|^{-1}\Bigg]. \quad (9)$$

Thus, as discussed above, sufficiently above the ionization thresholds the leading energy behavior of $\langle\psi_J|H-H_0|\psi_{2p_j\to J_\pm}\rangle$ is $E^{-1/2}$. From Eq. (9) this indicates the decreasing effect of the coupling on the relative phase shift going up in the energy. However, it is important to note here that this decay is much slower than $E^{-1/2}$ due to the logarithmic nature of the correction—a behavior that bears some consequence in the interchannel coupling effects on the photoelectron spin-polarization parameters.

Let us first focus on the effect of $2p_{1/2}$ channels on the spin polarization of $2p_{3/2}$ photoelectrons and *vice versa* (dotted curves). We compare between the thin solid curve (effectively the IP prediction) and the dotted curve of each of the

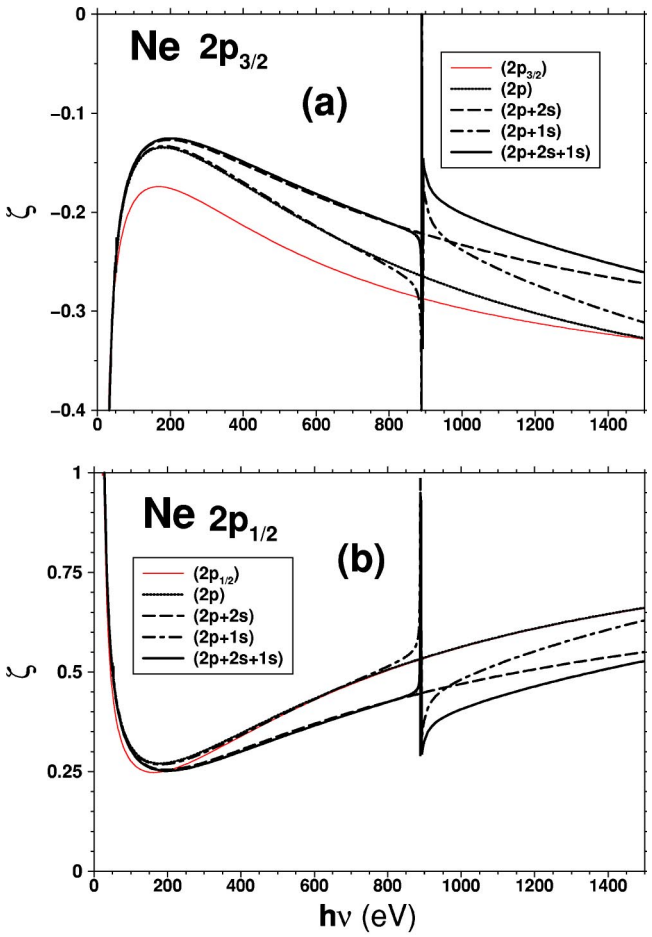


FIG. 4. Spin polarization parameter $\zeta$ for (a) $2p_{3/2}$ and (b) $2p_{1/2}$ photoelectrons.

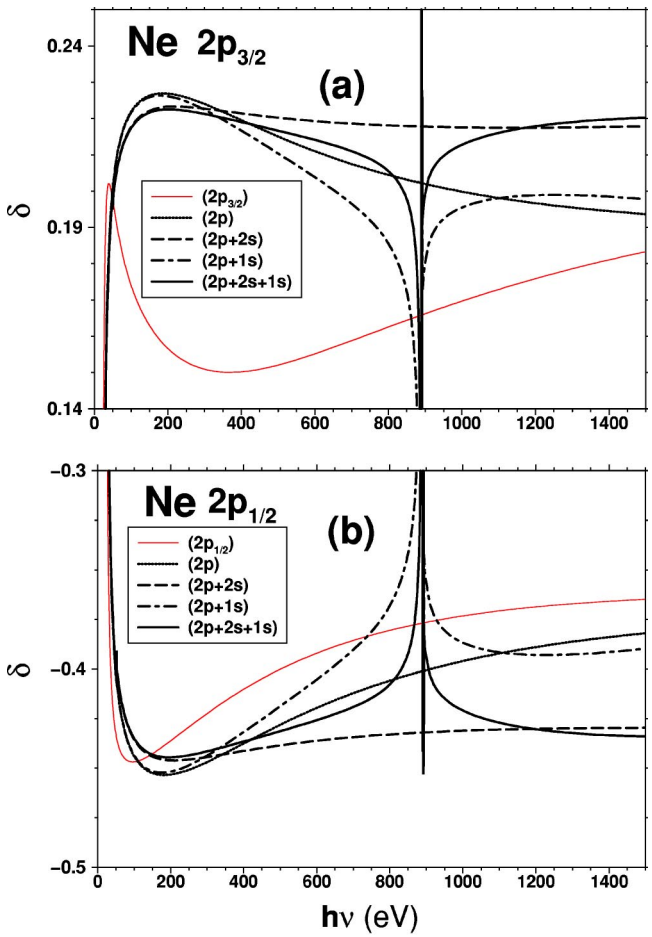


FIG. 5. Spin-polarization parameter $\delta$ for (a) $2p_{3/2}$ and (b) $2p_{1/2}$ photoelectrons.

Figs. 2–5. Evidently, for all the spin-polarization parameters the effect of this coupling is stronger at relatively low energies. This is clearly because the strength of the interchannel coupling matrix element decreases with increasing energy, as discussed above. But, as already made clear from the corresponding cross-section results, this coupling does not strongly affect the magnitude of the $2p_j$ dipole matrix elements. And since their unperturbed phases are nearly equal, the coupling does not alter their phases much [see Eq. (9)]. As a consequence, our results (not shown) of the angular distribution asymmetry parameter $\beta$, which depends on both the matrix elements and the phases, shows minimal effect of this coupling. But if the coupling affects neither the dipole matrix elements nor the phases significantly, how then can it affect the spin-polarization parameters? The answer lies in the fact that the values of the $2p_j$ spin-polarization parameters arise from complicated combinations of the dipole matrix elements and their phases, Eqs. (2)–(4), resulting in significant cancellations, so that small differences in dipole matrix elements and phases can be magnified to produce the results seen. The fact that the nonrelativistic limit of spin-polarization parameters are zero while for the $\beta$ parameter it is finite and close to its relativistic value indicates that such a cancellation mechanism is indeed operative for the spin-polarization parameters.

For all of the spin-polarization parameters, the result of this coupling, however, exhibits a rather slow monotonic tendency to converge to the corresponding effective IP-like prediction, with increasing energy, much slower than the convergence of the cross section. This is because the spin-polarization parameters depend upon phase shift differences as well, and these were shown above to converge more slowly than the magnitudes of the dipole matrix elements. This was also seen earlier in connection with $\beta$, which also depends on phase shifts [14]. Further, note that this coupling induces in general a stronger influence on the spin polarization of $2p_{3/2}$ electrons than on that of $2p_{1/2}$ electrons, except for $\eta$ (Fig. 3) where the results of both subshells have similar effect from this coupling. To provide some quantitative estimates, $\xi$ [Fig. 2(a)] and $\delta$ [Fig. 5(a)] for $2p_{3/2}$ electrons show, respectively, about 30% and 40% modification compared to the uncoupled results at roughly 300 eV photon energy; as expected, these differences decrease gradually as the energy increases. On the other hand, $\zeta$ for $2p_{1/2}$ electrons [Fig. 4(b)], which is related to the corresponding $\beta$ simply through $\zeta_{2p_{1/2}}=1-\beta_{2p_{1/2}}/2$, shows an almost negligible effect from this coupling.

Interchannel coupling of the $2p$ channels with either $2s$ or $1s$ channels involves alterations in both the magnitudes and phases of the $2p$ dipole matrix elements. Coupling with

the $2s$ channels affects the magnitudes of the $2p_{3/2}$ and $2p_{1/2}$ dipole matrix elements very strongly, as clearly indicated in Fig. 1. But the phases are also strongly affected [see Eq. (9)]. With the $1s$ coupling on the other hand, while the modifications to the magnitudes of the $2p_j$ dipole matrix elements are already small, except in a very small region around the $1s$ threshold, the alterations of the $2p_j$ phase shifts are also small. But it is nontrivial to assess in which direction the changes in these dynamical quantities, the magnitudes and the phases of the $2p_j$ dipole matrix elements, will induce changes in the spin-polarization parameters. For two of the spin-polarization parameters, $\xi$ (Fig. 2) and $\delta$ (Fig. 5), the effect of $2s$ and $1s$ coupling on $2p_j$ ionization is certainly not as straightforward as in the case of cross sections where only the magnitudes of the matrix elements (and not the phases) are important. In addition, by virtue of the different functional dependence of the parameters on the magnitudes of the dipole matrix elements and phase shifts, the qualitative behavior of the result changes from one parameter to another.

As seen in Fig. 2, the effect of $1s$ and $2s$ coupling on $2p_j$ for the parameter $\xi$ are roughly complementary until about 900 eV photon energy, the position of $1s$ Rydberg resonances; as a result, the deviation between the dotted (all $2p$ channels included) and thick solid (full calculation) results remains approximately constant. Beyond the resonance region the relative effect of $1s$ coupling drops off. However, over the entire energy range considered, the full calculation differs from the effective IP result (thin solid curve). This difference is significant for $2p_{3/2}$, showing a maximum alteration of about 25% at 300 eV, while for $2p_{1/2}$ the difference is rather small.

For parameters $\eta$ and $\zeta$, on the other hand, the $1s$ and $2s$ coupling influence the result quite in the similar qualitative manner as they do for the cross section. Along almost the complete energy range, albeit the near-threshold region (where interchannel coupling is known to be important), $\eta$ for both $2p_{3/2}$ and $2p_{1/2}$ [Figs. 3(a) and 3(b)] as well as $2p_{3/2}$ $\zeta$ [Fig. 4(a)] suggest an almost steady coupling contribution of more than 25% over the corresponding effective IP prediction. For $2p_{1/2}$ $\zeta$ [Fig. 4(b)], of course, the effect is small at lower energies, which, however, increases gradually with energy to yield over 20% correction.

The parameter $\delta$ (Fig. 5) being a combination of parameters $\xi$ and $\zeta$ exhibits a rather mixed behavior. For $2p_{3/2}$ photoionization [Fig. 5(a)] a maximum of 40% coupling effect is seen at around 300 eV that monotonically diminishes with increasing energy to eventually produce about 20% effect over the high energy range. For $2p_{1/2}$ [Fig. 5(b)] the effect of the coupling, which is weak at low energies, rises steadily to reach a value of about 20% at the highest energy considered.

These results clearly demonstrate that, as in the case of cross sections and angular distributions, the effect of interchannel coupling on the photoelectron spin polarization is considerable. However, due to the sensitivity of the spin polarization to relative phase shifts the results exhibit behavior that is qualitatively different from that of the cross-section results. While for the cross section, the high energy interchannel coupling effect generically increases going from lower to higher photon energies, for most of the spin-polarization parameters a strong coupling contribution appears already at low energies. As a consequence, a substantial coupling correction exists for these parameters over a very broad spectral range. Furthermore, coupling with $1s$ channels, which influences the cross section only over a narrow range, extends its influence over a much larger energy range for the $2p_j$ spin-polarization parameters owing to the much slower drop-off of the phase-shift corrections induced by interchannel coupling. Finally, we note that although we have illustrated the effect with an example of valence photoionization of Ne, the same mechanism of configuration interactions in the *continuum* (interchannel coupling) must be operative for the spin polarization of photoejected electrons from any arbitrary atom or atomic ion and from any subshell.

## IV. CONCLUSION

It is shown in this paper that the photoelectron spin polarization of an atom is strongly influenced by the electron correlation via interchannel coupling over the entire spectral range. Unlike to the cross section, where only the coupling-induced alteration of the magnitudes of matrix elements is responsible for the behavior, modification of the phase shifts plays an important role determining the effect on the spin polarization. For the cross section and the angular distribution the importance of interchannel coupling for energetic photoemission has been demonstrated previously [14]. With the current result we conclude, therefore, that in order to acquire a *complete* knowledge of photoionization dynamics unambiguously over the range from vuv all the way to hard x-rays, theoretical study including the interchannel coupling is absolutely required.

## ACKNOWLEDGMENTS

This work was partly supported by NSF, NASA, and DST India. The authors are grateful to Walter Johnson, University of Notre Dame, for the use of his RRPA code. H.S.C. acknowledges the computer time from the Department of Physics and Astronomy, GSU, Atlanta.

[1] E.W.B. Dias, H.S. Chakraborty, P.C. Deshmukh, and S.T. Manson, J. Phys. B **32**, 3383 (1999).
[2] V. Radojevic and J.D. Talman, J. Phys. B **23**, 2241 (1990).
[3] B. Kämmerling and V. Schmidt, Phys. Rev. Lett. **67**, 1848 (1991); J. Phys. B **26**, 1141 (1993).
[4] G. Snell, U. Hergenhahn, N. Müller, M. Drescher, J. Viefhaus, U. Becker, and U. Heinzmann, Phys. Rev. A **63**, 032712 (2001).
[5] U. Fano, Phys. Rev. **178**, 131 (1969).
[6] N.A. Cherepkov, Adv. At. Mol. Phys. **19**, 395 (1983).
[7] U. Heinzmann and N.A. Cherepkov, in *VUV and Soft X-Ray Photoionization,* edited by U. Becker and D.A. Shirley (Ple-

num, New York, 1996).
[8] H.A. Bethe and E.E. Salpeter, *Quantum Mechanics of One- and Two-Electron Atoms* (Springer-Verlag, Berlin, 1958), Sec. 71.
[9] W. Cooper, in *Atomic Inner-Shell Processes*, edited by B. Crasemann (Academic Press, New York, 1975), Vol. 1, p. 170.
[10] S.T. Manson and D. Dill, in *Electron Spectroscopy: Theory, Technique and Applications*, edited by C.R. Brundle and A.D. Baker (Academic Press, New York, 1978), p. 186.
[11] J. Berkowitz, *Photoabsorption, Photoionization and Photoelectron Spectroscopy* (Academic Press, New York, 1979), p. 61.
[12] A.F. Starace, in *Handbuch der Physik*, edited by W. Mehlhorn (Springer-Verleg, Berlin, 1982), Vol. 31, p. 46.
[13] A.F. Starace, in *Atomic, Molecular, & Optical Physics Handbook*, edited by G.W.F. Drake (AIP Press, Woodbury, New York, 1996), p. 305.
[14] E.W.B. Dias, H.S. Chakraborty, P.C. Deshmukh, S.T. Manson, O. Hemmers, P. Glans, D.L. Hansen, H. Wang, S.B. Whitfield, D.W. Lindle, R. Wehlitz, J.C. Levin, I.A. Sellin, and R.C.C. Perera, Phys. Rev. Lett. **78**, 4553 (1997).
[15] D.L. Hansen, O. Hemmers, H. Wang, D.W. Lindle, P. Focke, I.A. Sellin, C. Heske, H.S. Chakraborty, P.C. Deshmukh, and S.T. Manson, Phys. Rev. A **60**, R2641 (1999).
[16] H.S. Chakraborty, D.L. Hansen, O. Hemmers, P.C. Deshmukh, P. Focke, I.A. Sellin, C. Heske, D.W. Lindle, and S.T. Manson, Phys. Rev. A **63**, 042708 (2001).
[17] W.R. Johnson and C.D. Lin, Phys. Rev. A **20**, 964 (1979).
[18] W.R. Johnson, C.D. Lin, K.T. Cheng, and C.M. Lee, Phys. Scr. **21**, 409 (1980).
[19] K.-N. Huang, W.R. Johnson, and K.T. Cheng, Phys. Rev. Lett. **43**, 1658 (1979).
[20] K.-N. Huang, Phys. Rev. A **22**, 223 (1980).
[21] U. Fano and A.R.P. Rau, *Atomic Collisions and Spectra* (Academic Press, Orlando, 1986), p. 66.
[22] From this very simple argument it is easy to show that the full partial cross section for any $nl(l>0)$ photoionization will always behave as $E^{-9/2}$ in the limit $E\rightarrow\infty$ owing to the interaction with nearby $nl$ $(l=0)$ channels. This corresponds to a part of the result obtained in Ref. [23].
[23] M.Ya. Amusia, N.B. Avdonina, E.G. Drukarev, S.T. Manson, and R.H. Pratt, Phys. Rev. Lett. **85**, 4703 (2000).